C. Kuang
Central Iron & Steel research Institute
Advanced Technology & Materials Corp.
100081, Beijing, P.R.China
kcjwxx@btamail.net.cn
Fax: 0086-10-62182530

J. Zhang
Beijing University of Chemical Technology
100029, Beijing, P.R.China
zhangjw@netease.com
Telephone:0086-10-64434789
Fax: 0086-10-64437587

F. Wang
Advanced Technology & Materials Corp.
100081, Beijing, P.R.China
wfnice@sina.com
Telephone:0086-10-62182381
Fax: 0086-10-62182530

J. Chen
Beijing University of Chemical Technology
100029, Beijing, P.R.China
chenjf@netease.com
Telephone:0086-10-64434789
Fax: 0086-10-64437587

Development and Behavior of Metallic Filter Element and Numerical Simulation of Transport Phenomena during Filter Regeneration Process*

Keywords: Hot gas filtration, Metallic filter elements, Pulse-jet cleaning, Numerical simulation

1. Introduction

Gas filtration at high temperature from industrial processes offers various advantages in terms of increasing process efficiency, improving recovery of heat and materials resources, protection of downstream plant equipments, and at the same time it is an advanced environmental protection technology. Gas filtration at high temperatures has great potential applications in various industrial fields, such as Integrated Gasification and Combined Cycle (IGCC) power generation process, chemical and petrochemical industry, Ironmaking and Steelmaking processes, ceramic industry and incinerator units, etc. (Shi 1997, Peukert 1998 and Xia 1999).

Of the available filtration methods, barrier filters (ceramic filters, metallic filters, etc.) are thought to be the most promising devices for hot gas cleaning in their utmost utilization of hot gas energy, in process investment saving and in elimination of secondary water pollution occurred with a wet scrubber process. Since 1970's, great efforts have be made to develop advanced filter elements and high temperature filtration technology, with the aim mainly to put the advanced coal-based power generation systems such as pressurized bed combustion (PFBC) and integrated gasification combined cycle (IGCC) into commercial application. The US Department of Energy (DOE) has launched serials of lab-scale to industry-scale research programs to develop high temperature gas filtration technology with ceramic filter elements, and same work has been done in other developed countries, such as in Germany, Japan and England, etc. (Rubow et al. 1984, Krein 1999; Oda et al. 1996, Chalupnick et al. 1999 and Dennis et al. 1999). Great progress has since then been made in advanced filter elements development and filtration technology development, including some sintered metallic filter elements, such as sintered metallic filter tubes of 310S, Inconel 600, FeAl intermetallic

* *The project was supported by China national natural science foundation, Grant No. 50074027*

materials from Mott and Pall corporation, with temperature resistance up to 600 -900℃ (Alvin 1999, Sawada 1999 and Sunil et al. 1999).

Since 1990s, the Chinese Ministry of Science and Technology has launched research programs to solve the problem of sulfur species and particulate's polishing in hot gas, with the aim to realize the commercialization of IGCC process and to develop the country's advanced coal-based power generation technology. The Central Iron & Steel Research Institute (CISRI)/AT&M Corp. and some other research institutions took up the research project of experimental investigations on high temperature gas filtration technology, including development of advanced filter elements, investigation of pulse-jet cleaning, design and development of high temperature filter device and pilot-scale experiment of hot gas filtration. This paper describes some of the research results in the development of advanced filter elements and hot gas filtration technology, and in numerical simulation of transport phenomena in hot gas filtration processes.

.

2. Objectives and Approach

Ceramic filters have revealed to have good thermal resistance and chemical corrosion resistance, but they are brittle and lack of toughness, and liable to rupture under large temperature swings. Metallic filters with their high strength and toughness and good heat conduction ability have showed good thermal shock resistance, 310S and FeAl intermetallic filter elements have exhibited additionally good chemical corrosion resistance in oxidizing and sulfidizing atmosphere(Sawada 1999 and Sunil et al. 1999). The behavior of metallic filter elements at high temperature was investigated and the filtration efficiency of the filter units for hot gas from a coal gasifier unit was tested.

Pulse-jet cleaning of filter elements is a key component in the operation of the filtration unit. The pulse-jet is introduced into the filter element cavities from the clean side, and the dust cakes on the outer surfaces of the filter elements are detached and fall into the filter vessel. Sequential on-line cleaning of filter element groups yields a filter operation with no shut-down for filter regeneration. Development of advanced technologies in the design and operation of the pulse cleaning is one of the important tasks in order to increase the system reliability, to improve the filter life and to increase the filtering performance. A great deal of theoretical and experimental research works have be done in order to investigate the regeneration mechanism of filter elements and to optimize the design of pulse cleaning system (Choi 1999, Kanoka 1999, Grannel et al. 1999, Ferer et al. 1999 and Ji et al. 1999). The regeneration of filter element in gas filtration at high temperature plays a very important role for the operation of the process. Based on experimental observation and field operation, a numerical model is set up to numerically simulate the momentum and heat transport phenomena in the regeneration process, which is essential for understanding of the process, the optimization of process parameters and improvement of the design of the structure of venturi nozzle and the configuration of the apparatus.

3. Project Description

3.1 Description of the hot gas filtration tests

The hot gas filtration tests were carried out at a pilot-scale coal gasifier unit. Sintered metal mesh filter elements of 310S materials developed by AT&M Corp. was used in the experiment. The filter system adopted the pulse-jet cleaning technology, and nitrogen gas with a pressure about 2 MPa was used as cleaning gas. The filtration process was shown in Fig.1. After two stages of cyclone filtration, raw gas from coal gasifier with temperatures about 600^{o}C was introduced into the filter. The parameters for the experiment are given in table 1.

3.2 Model Description

The cleaning of dust deposit by reverse pulse cleaning is an unsteady process. Based on this consideration, the numerical simulations have been performed for the transient development of the pulse cleaning process.

3.2.1 Governing equations in two-dimensional cylinder coordinate system for internal candle

1) Continuity Equation

$$\frac{\partial}{\partial t}(\rho)+\frac{\partial}{\partial z}(\rho w)+\frac{1}{r}\frac{\partial}{\partial r}(r\rho v)=0 \tag{1}$$

2) Axial Momentum Equation

$$\frac{\partial}{\partial t}(\rho w)+\frac{\partial}{\partial z}(\rho w w)+\frac{1}{r}\frac{\partial}{\partial r}(r\rho v w)=\frac{\partial}{\partial z}(\mu_{eff}\frac{\partial w}{\partial z})+\frac{1}{r}\frac{\partial}{\partial r}(r\mu_{eff}\frac{\partial w}{\partial r})+S_w \tag{2}$$

where $\mu_{ef}=\mu+\mu_t$ $\quad S_w=-\frac{\partial P}{\partial z}+\frac{\partial}{\partial z}(\mu_{eff}\frac{\partial w}{\partial z})+\frac{1}{r}\frac{\partial}{\partial r}(r\mu_{eff}\frac{\partial v}{\partial z})+\rho g$

3) Radial Momentum Equation

$$\frac{\partial}{\partial t}(\rho v)+\frac{\partial}{\partial z}(\rho w v)+\frac{1}{r}\frac{\partial}{\partial r}(r\rho v v)=\frac{\partial}{\partial z}(\mu_{eff}\frac{\partial v}{\partial z})+\frac{1}{r}\frac{\partial}{\partial r}(r\mu_{eff}\frac{\partial v}{\partial r})+S_v \tag{3}$$

where $\quad S_v=-\frac{\partial P}{\partial r}+\frac{\partial}{\partial z}(\mu_{eff}\frac{\partial w}{\partial r})+\frac{1}{r}\frac{\partial}{\partial r}(r\mu_{eff}\frac{\partial v}{\partial r})-\frac{2\mu_{eff}v}{r^2}$

4) Energy equation

$$\frac{\partial}{\partial t}(\rho T)+\frac{\partial}{\partial z}(\rho w T)+\frac{1}{r}\frac{\partial}{\partial r}(r\rho v T)=\frac{\partial}{\partial z}(\Gamma\frac{\partial T}{\partial z})+\frac{1}{r}\frac{\partial}{\partial r}(r\Gamma\frac{\partial T}{\partial r})+S_T \tag{4}$$

in which, $\Gamma=\frac{\mu}{\mathrm{Pr}}+\frac{\mu_t}{\sigma_T}$ $\quad S_T=0$

3.2.2 Turbulence model

Turbulence model of *k*-ε two-equation is adopted in this paper. The isotropic assumption of turbulence is appropriate. In order to treat the transport phenomena adjacent to the wall, the wall function method is used for the region adjacent to the walls.

5) Turbulent kinetic energy equation

$$\frac{\partial}{\partial t}(\rho k)+\frac{\partial}{\partial z}(\rho w k)+\frac{1}{r}\frac{\partial}{\partial r}(r\rho v k)=\frac{\partial}{\partial z}(\Gamma\frac{\partial k}{\partial z})+\frac{1}{r}\frac{\partial}{\partial r}(r\Gamma\frac{\partial k}{\partial r})+S_k \tag{5}$$

where $\Gamma=\mu+\frac{\mu_t}{\sigma_k}$, $S_k=G-\rho\varepsilon$

6) Dissipation rate of turbulence kinetic energy

$$\frac{\partial}{\partial t}(\rho\varepsilon)+\frac{\partial}{\partial z}(\rho w\varepsilon)+\frac{1}{r}\frac{\partial}{\partial r}(r\rho v\varepsilon)=\frac{\partial}{\partial z}(\Gamma\frac{\partial\varepsilon}{\partial z})+\frac{1}{r}\frac{\partial}{\partial r}(r\Gamma\frac{\partial\varepsilon}{\partial r})+S_\varepsilon \tag{6}$$

in which, $\Gamma=\mu+\frac{\mu_t}{\sigma_\varepsilon}$, $S_\varepsilon=\frac{\varepsilon}{k}(c_1G-c_2\rho\varepsilon)$

$$\mu_t=c_\mu\frac{\rho k^2}{\varepsilon} \tag{7}$$

where, C_1, C_2, C_μ, σ_k, σ_ε are model constants. *G* is the Generation rate of momentum. And in two dimensional cylinder coordinate system, G can be written as:

$$G=\mu_t\{2[(\frac{\partial w}{\partial z})^2+(\frac{\partial v}{\partial r})^2+(\frac{v}{r})^2]+(\frac{\partial w}{\partial r}+\frac{\partial v}{\partial z})^2\} \tag{8}$$

3.2.3 Governing equations in two dimensional cylinder coordinates system in porous region

1) Continuity Equation

$$\frac{\partial}{\partial t}(\varepsilon_{\mathrm{P}}\rho)+\frac{\partial}{\partial z}(\varepsilon_{\mathrm{P}}\rho w)+\frac{1}{r}\frac{\partial}{\partial r}(\varepsilon_{\mathrm{P}} r\rho v)=0 \tag{9}$$

2) Axial Momentum Equation

$$\frac{\partial}{\partial t}(\varepsilon_{\mathrm{P}}\rho w)+\frac{\partial}{\partial z}(\varepsilon_{\mathrm{P}}\rho w w)+\frac{1}{r}\frac{\partial}{\partial r}(\varepsilon_{\mathrm{P}} r\rho v w)=-\varepsilon_{\mathrm{P}}\frac{\partial P}{\partial z}+\frac{\partial}{\partial z}(\varepsilon_{\mathrm{P}}\mu\frac{\partial w}{\partial z})+\frac{1}{r}\frac{\partial}{\partial r}(\varepsilon_{\mathrm{P}} r\mu\frac{\partial w}{\partial r})+\rho g\varepsilon_{\mathrm{P}} \tag{10}$$

3) Radial Momentum Equation

$$\frac{\partial}{\partial t}(\varepsilon_{\mathrm{P}}\rho v)+\frac{\partial}{\partial z}(\varepsilon_{\mathrm{P}}\rho w v)+\frac{1}{r}\frac{\partial}{\partial r}(\varepsilon_{\mathrm{P}} r\rho v v)=-\varepsilon_{\mathrm{P}}\frac{\partial P}{\partial r}+\frac{\partial}{\partial z}(\varepsilon_{\mathrm{P}}\mu\frac{\partial v}{\partial z})+\frac{1}{r}\frac{\partial}{\partial r}(\varepsilon_{\mathrm{P}} r\mu\frac{\partial v}{\partial r}) \tag{11}$$

4) Energy equation in porous media

$$\frac{\partial}{\partial t}[\varepsilon_{\mathrm{P}}\rho_f+(1-\varepsilon_{\mathrm{P}})\rho_S\frac{C_{PS}}{C_{Pf}}]T+\frac{\partial}{\partial z}(\varepsilon_{\mathrm{P}}\rho_f wT)+\frac{1}{r}\frac{\partial}{\partial r}(\varepsilon_{\mathrm{P}} r\rho_f vT)=\frac{\partial}{\partial z}(\Gamma\frac{\partial T}{\partial z})+\frac{1}{r}\frac{\partial}{\partial r}(r\Gamma\frac{\partial T}{\partial r}) \tag{12}$$

in which, $\Gamma=\varepsilon_{\mathrm{P}}\dfrac{\mu_f}{\mathrm{Pr}_f}+(1-\varepsilon_{\mathrm{P}})\dfrac{k_S}{C_{\mathrm{pf}}}$.

3.2.4 Model constants

The values of the model constants are as follows (Joseph et al. 1994):

C_1=1.44 C_2=1.92 C_μ=0.09 σ_k=1.0 σ_ε=1.3 σ_T=0.9

3.2.5 Computational Domain

Due to the axisymmetry of the system, half of the radial field is needed to study. The calculation domain includes the cleaning lance, the porous metal grid element and the venturi as shown in Fig.3. The computational domain is discriticized into meshes: in z direction about 110 cells, in r direction about 30 cells. All the cells in z direction and r direction are uniform respectively.

3.2.6 Boundary conditions

Fluid conditions:

Axial direction:

Inlet z=0

w=187 m s^{-1}, v=0 m s^{-1} , T=387 K, k_{in}=10^{-4}W$_{\mathrm{in}}^2$, $\varepsilon_{\mathrm{in}}$=0.1643 $k_{\mathrm{in}}^{1.5}$/0.1D

Close end z=H

w=0.0, $\dfrac{\partial\phi}{\partial z}=0$ (=v, k, ε , T)

All properties of the fluid are calculated dependant on temperature.

Radial direction

r=0: v=0.0, $\dfrac{\partial\phi}{\partial r}=0$ (=w, k, ε , T)

r=R: w=0.0, $\dfrac{\partial\phi}{\partial r}=0$ (=v, k, ε , T)

Properties of porous media:

Porosity: ε_{P}=0.35

Permeability: K=5.56×10^{-11} m^2

Thermal conductivity: k_{S}=20 W·m^{-1}·K^{-1}

3.2.7 Initial Conditions

Since the process is very short for at about second order, immediately after the starting of the pulse jet cleaning, the turbulent jet gas flow mixes with the surrounding gas which is initially stationary. Thence it comes the problem how to deal with the sudden transition for the surrounding gas from initial static condition to the turbulent conditions disturbed by the pulse jet. In this paper, initial conditions for turbulent kinetic energy and the dissipation rate of turbulent kinetic energy are set as 10^{-4} w_{in}^2 and 0.1643 $k_{in}^{1.5}$/0.1D respectively, where w_{in} and D is the value of axial velocity at the lance outlet and lance diameter respectively.

4. Results and discussion

4.1 Experimental Results

Fig.3 shows the variation of the operation data, such as gas flow rate, filter pressure drop and inner wall temperature of filter vessel during filtration operation. The filter system operated stable, with temperature oscillation less than 5 ~ 10ºC, gas flow rate oscillation less than 5~10 % and system pressure oscillation less than 5%. The pulse-jet cleaning system worked well. The pressure drop of the filter elements recovered to the original pressure drop value after cleaning. When the filter pressure drop was kept under 15 ~ 30Kpa, the cleaning cycle was about 15 ~ 60 min. The pilot-scale experiment achieved a filtration efficiency greater than 99.9%, with dust load of purified gas less than 5mg/Nm^3.

4.2 Numerical Results

The above conservation equations are discritized and SIMPLEC method (Van Doormaal et al. 1984) is adopted to solve the discritized conservation equations. During the calculation, Great attentions are paid on the relaxing factors to obtain good convergence.

For the simulation of the filtration and regeneration processes during hot gas filtration, the effect of some parameters including the distance between the jet lance and the venturi, the jet velocity and the permeability of the porous metal grid are studied here. Since a secondary flow is induced at the region of top venturi by the air jet, which causes severe difficulties to achieve convergence of numerical simulation, small relaxing factors for velocity components and pressure are used to avoid divergence. The entrainment of surrounding gas by pulse jet, the distribution of pressure along axial direction and radial direction, the development of the pulse jet along the axial direction and the transverse radial direction, the flow structure as well as the flow rates of air at different axial positions are illustrated. Also found by our numerical simulation is the unsteady pressure oscillation reported by Grannell and Seville (1999). Although the detachment of dust cake is not discussed due to insufficient information of dust layer, the numerical simulation may direct the improvement of the design of the structure of venturi and the configuration of the apparatus. The numerical simulation is shown in Fig.4 to 12 and will be described in three subsections.

4.2.1 Effect of different distances between jet nozzle and the venturi H on the flow structure

A secondary vortex forms in the region adjacent to the ventrui left-top corner. Due to the suction of pulse jet out of the jet lance, the gas is suctioned into the jet body. With the expansion of the jet, the interaction between the jet body and the suctioned gas flow leads to the above vortex. The axial velocity component for three different H can be seen in Figure 4.

It is very important to know the entrainment amount of jet cleaning, since the amount of entrainment plays a key role in the cleaning efficiency. Figure 5 shows the variation of entrainment amount vs tme evolution sequence. It can be seen that the jet flow almost achieves a pesudo-steady state after about 0.18~0.36 s. And during the pesudo-steady state, the entrainment achieves the greatest value just before the venturi. After entering the venturi, the entrainment amount keeps almost unchanged. The final amount entering the candle is

about 2.8 times the inflow of jet from reservoir. On the other hand, it is obvious that the entrainment of jet is not used completely, i.e. part of the entrainment loses due to an unappropriate construction conditions set by this numerical simulation. This also indicates a direction for improvement of the structure of ventrui, the configuration of the apparatus. This also indicates a direction for improvement of the structure of ventrui, the configuration of the apparatus. Further research work will come soon. From this figure, it may be deduced that the approciate distance H should be within the range from 2.5 to 7.5 cm. The pressure distribution and flow structure for different H can be seen in Figure 6-7.

4.2.2 Effect of different inlet axial velocity on the flow structure
The results of transient entrainment of gas for different inlet velocity can be seen in Figure 8. The great difference between the results of 50m/s and 120m/s and 187m/s is clear. The results of transient entrainment of gas for different inlet axial university can be seen in Figure 9.

4.2.3 Effect of different permeability on the flow structure
The results of flow structure for different permeability of porous metal grid are shown in Figure 10 and 11. There is not signifficant difference between the two cases. The flow field can achieve pesudo-steady state for smaller porosity.

4.2.4 Thermal structure
The results of thermal structure under pesudo-steady state for different distance of H between jet nozzle and venturi are given in Figure 12. It can be seen at most cases, mainly the region from the nozzle to the venturi is effected by the coming cooler air. The temperature difference lies in the region around the venturi. This phenomena may be important and design for the filter at high temperature.

5 Conclusions
1) Metallic filter elements, such as sintered 310S and Fe_3Al intermetallics, are promising candidates to be used in commercial hot gas filtration units.
2) A stable and high efficient hot gas filtration operation has been achieved with sintered metal filter elements, the particulate emission in gas was less than 5 ppm.
3) A model is setup to numerically simulate the momentum and heat transport in a pulse jet gas cleaning process at high temperature. The numerical results reveal the development of the pulse jet along the axial direction and transverse the radial direction.
4) The numerical simulation found the approciate distance between the nozzle and the venturi may be within 2.5 cm to 7.5 cm for the case studied. And also found is the negative pressure pore as is usually met in jet flow. By numerical simulation, it can be deduced that the regeneration by pulse jet would achieve a pesudo-steady state at about 0.18~0.356 s after the initiation of cleaning. It is found mainly the temperature in the region from the nozzle to the venturi is effected by the coming air.

Nomenclature

C_P	specific heat, J/kg·K
D	diameter, m
g	gravity accelerator, $m \cdot s^{-2}$
H	distance between the lace jet and the venturi, m
k	turbulence kinetic energy, $J \cdot s^{-1}$, thermal conductivity, $W \cdot m^{-1} \cdot K^{-1}$
K	permeability, m^2
Q	volume flow rate of gas, $m^3 \cdot s^{-1}$

r	radial coordinate, m
R	radius, m
S	source term
t	time, s
T	temperature, K
v	radial velocity component, $m \cdot s^{-1}$
w	axial velocity component, $m \cdot s^{-1}$
z	axial coordinate, m

Greek sysmols

Γ	general diffusivity, $m^2 \cdot s$
μ	dynamic viscosity, Pa·s
ρ	Density, $kg \cdot m^{-3}$
ε	dissipation rate of turbulent energy,
ε_P	porosity of metal region
ϕ	generalized variable

Subscript

f	fluid
s	metal grid
t	turbulence

References

Alvin M.A., 1999. Hot gas filter development and performance, *High Temperature Gas Cleaning, Volume II*, Edited by A.Dittler, G.Hemmer, G.Kasper, 455.

Chalupnick R., Isaksson J., Jones B., Krein J., Koebernick O., Schulz K., 1999. Demonstration of hot gas filtration systems, *High Temperature Gas Cleaning, Volume II*, Edited by A.Dittler, G.Hemmer, G.Kasper: 276.

Choi J.H., 1999. Investigation into the pulse cleaning of the ceramic filter candle. *High Temperature Gas Cleaning, Volume II*, Edited by A.Dittler, G.Hemmer, G.Kasper: 541.

Dennis R., McMahon T., Dorchak T., Chiang T., 1999. U.S. Department of energy's high-temperature and high-pressure particulate cleanup program for advanced coal-based power systems, *High Temperature Gas Cleaning, Volume II*, Edited by A.Dittler, G.Hemmer, G.Kasper: 303.

Ferer M., Duane H. Smith, 1999. A simple model of filter cake removal, High temperature gas cleaning. Volume II, Edited by A. Dittler, G. Hemmer, G. Kasper: 172.

Grannel S.K. and Seville J.P.K., 1999. Effect of venturi inserts on pulse cleaning of rigid ceramic filters, *High Temperature Gas Cleaning, Volume II*, Edited by A.Dittler, G.Hemmer, G.Kasper: 96.

Gross R., Hecken M., Renz U., 1998. Hot gas filtration with ceramic filter candles: Experimental and numerical investigations on fluid flow during element cleaning: 862-873.

Ji Z., Meng X., Shi M., Ding F., 1999. The interim process between pulse-backing cleaning and normal filtration processes of ceramic filter, *High Temperature Gas Cleaning, Volume II*, Edited by A.Dittler, G.Hemmer, G. Kasper: 211.

Joseph H.W. Lee, Wolfgang Rodi, 1994. Numerical simulation of line puffs, in Recent

research advances in the fluid mechanics of turbulent jets and plumes. P.A. davies, M. J. Valene Neves eds, Kluwer Academic Publishers, Netherlands: 73-88.

Kanoka C., Amornikitbamrung A. and Kishima T., 1999. Cleaning mechanism of dust from ceramic filter element. *High Temperature Gas Cleaning, Volume II*, Edited by A.Dittler, G.Hemmer, G. Kasper: 142.

Krein J., 1999. LLB Candle filter for the ELCOGAS IGCC power plant Puertollano /Spain, High temperature gas cleaning. Volume II, Edited by A.Dittler, G.Hemmer, G.Kasper: 253.

Kuang C.J., Fang Y.C., Gu. L. and Wang Y.C., 1999. Metal porous materials and its application in cleaning of gasous aerosol, 7 th National Conference on Aerosol, Xi'an.

Oda N.and Hanada T., 1996. Performance of the advanced ceramic tube filter (ACTF) for the Wakamatsu 71 Mw PFBC and further improvement for commercial Plants. Proc. of 3rd Int. Symp. On gas cleaning of high temperature, Karlsruhe, Germany.

Peukert W., 1998. High temperature filtration in the process industry. *Filtration & Separation:* 461.

Rubow L.N, Zaharchuk R. 1991. Results of technical and economic evaluation of ten high-temperature and high-pressure particulate cleanup systems for PFBC, DOE/MC/ 19196-1654, p304. 1984 (NTIS/DE84012004) M.J.Mudd, etc. American electric power's PFBC hot gas clean up test program, Proc. of 11th Int. Conf. on FBC, ASME: 953.

Sawada Y., K. Hiramatsu, H.Kawamoto, etc. 1999. Evaluation on fundamental pro-perties of filter materials at high temperature, *High Temperature Gas Cleaning, Volume II*, Edited by A.Dittler, G.Hemmer, G.Kasper: 393.

Shi M.X., 1997. Modern development of Gas Filtration at High Temperature. Proceedings of 5th heterogenuous separat on, Beijing.

Sunil Jha, Ronald S.sekellick and Kenneth L.Rubow, 1999. Sintered metal hot gas filters, *High temperature gas cleaning, Volume II*, Edited by A.Dittler, G.Hemmer, G.Kasper: 492.

Van Doormaal J.P. and Raithy G.D., 1984. Enhancement of the SIMPLE method for predicting incompressible fluid flows. *Numerical Heat Transfer* 7: 147-163.

Xia, X.X. 1999. Review of Gas Filtration at High Temperature. Proceedings of 6 th heterogenuous separation, Beijing.i

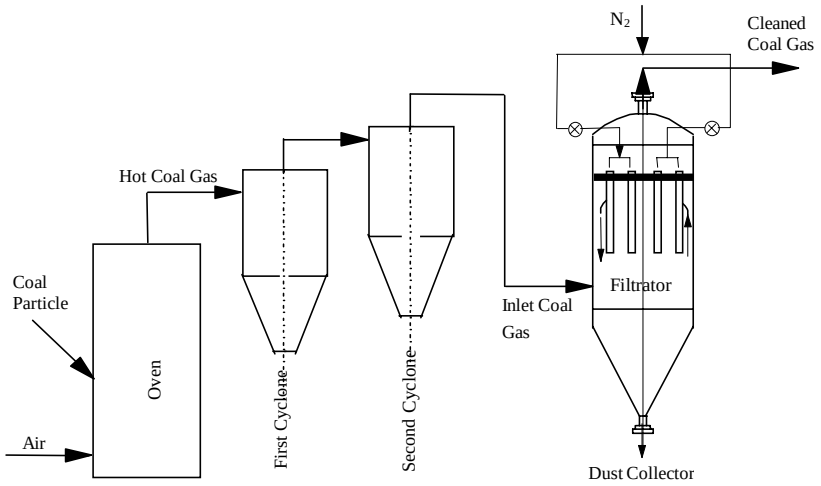

Fig.1 Flowsheet of coal gasification and hot gas filtration process

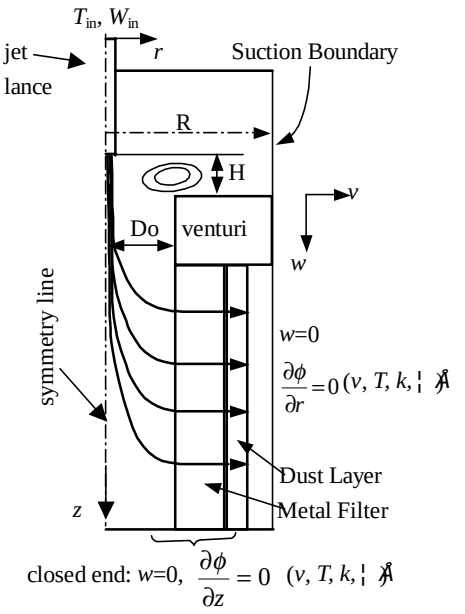

Fig.2 Schematic show of Gas Cleaning at High Temperature

Table 1 Hot gas operating conditions

Working conditions		Filter characteristics	
Temperatures ^{o}C	580 – 620	Size and number	Φ50x1000 mm x 6
Pressure MPa	1.0 – 1.1	Filtration ratio	20 μm
Gas flow rate Nm^3/h	130 – 220	Porosity	35%
Dust content mg/Nm^3	3500 – 9500	Gas permeability	3.10^{-3}l/cm^2.min.pa
Particle sizes d_{50}/d_{90}, μm	5.2/10	Weight of each element	2 Kg
Gas composition %	CO ~20，CO_2 ~15，N_2 ~50，H_2O ~10		

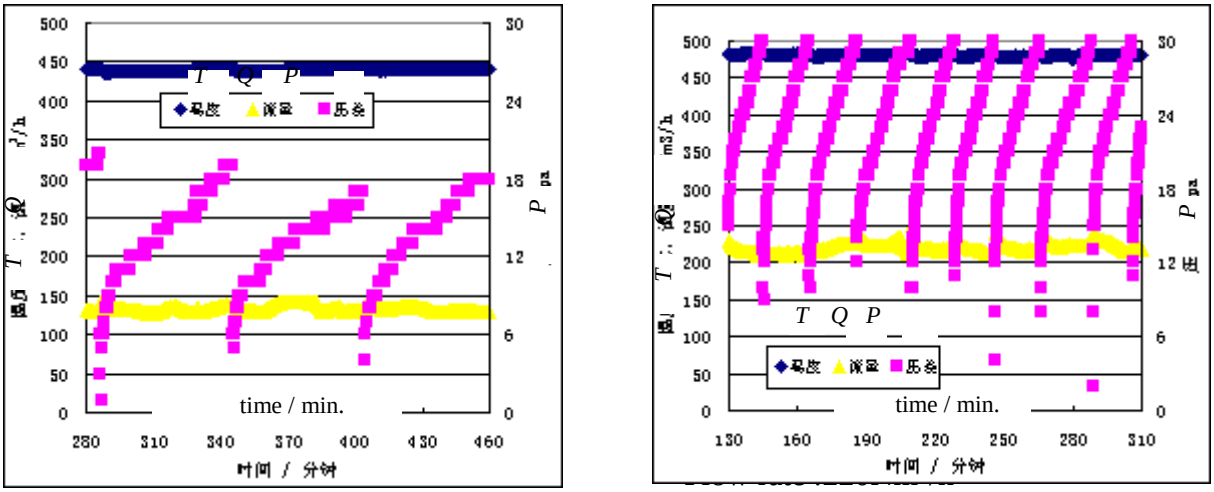

Figure 3 Change of pressure drops and temperatures during hot gas filtration

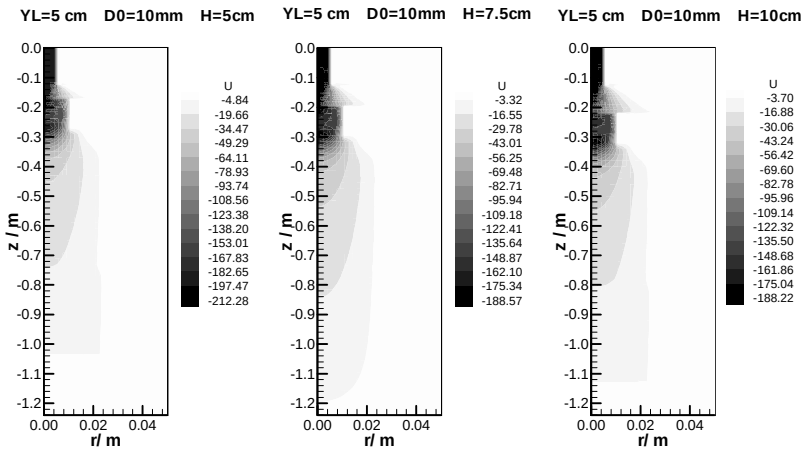

Figure 4 Pesudo-steady flow structure for three different distances H

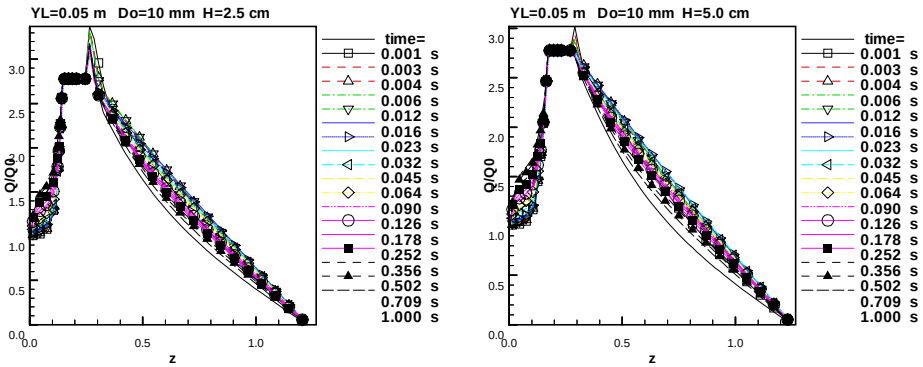

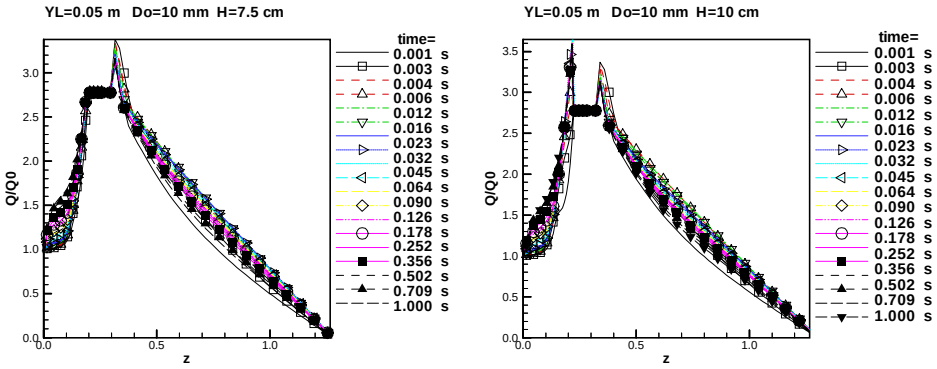

Figure5 Transient entrainment of gas for different distances H

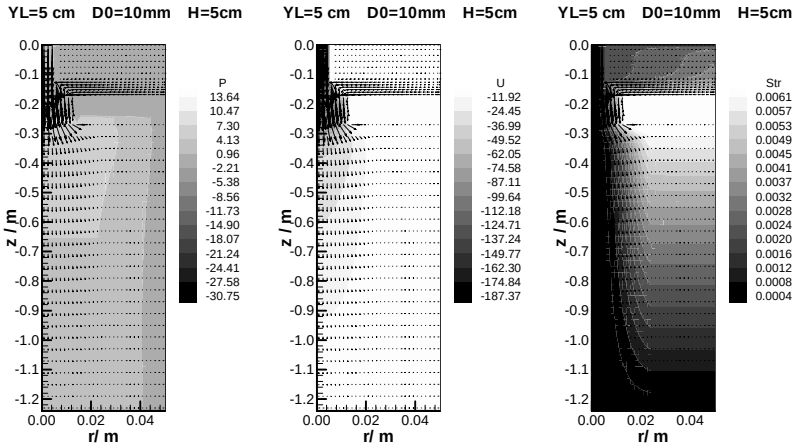

Figure 6 Results of flow structure for H=5.0 cm at t=0.356 s

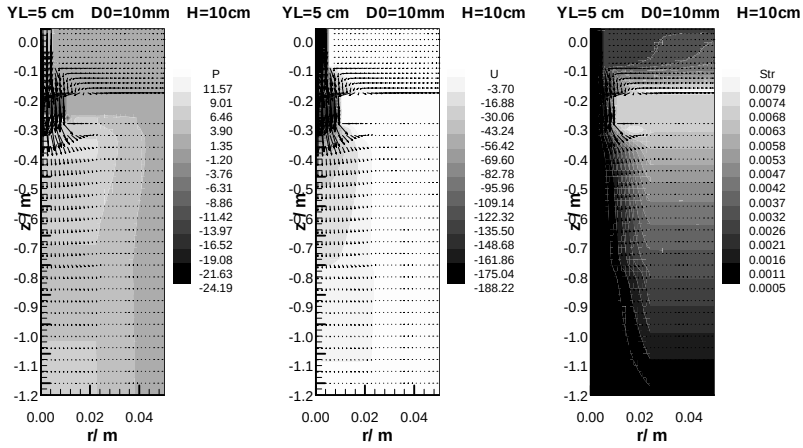

Figure 7 Flow structure for H=10cm at t=0.356 s

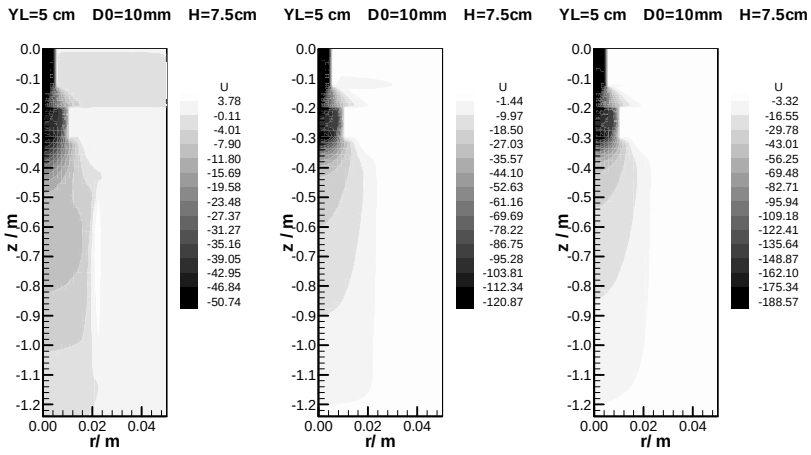

Figure 8 Flow structure for H=7.5 cm at t=0.356 s

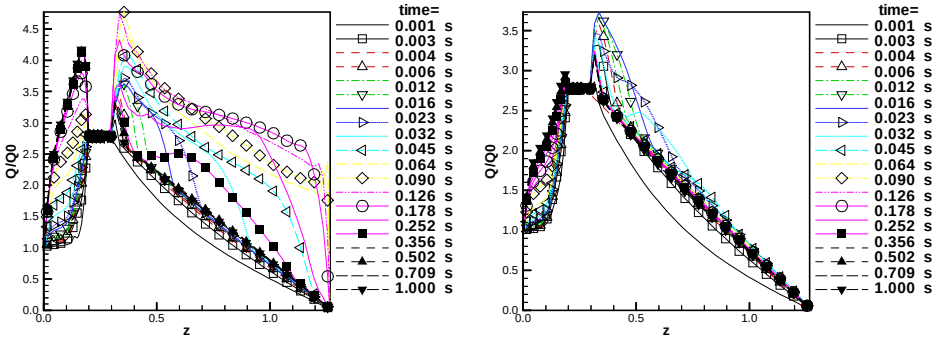

Figure 9 Transient entrainment of gas for different axial inlet velocities (Left: 50m/s Right: 120 m/s)

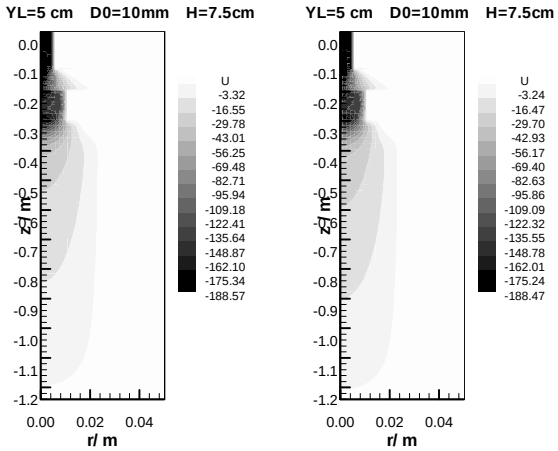

Figure 10 Flow structure for different permeability (Left: $5.56\times10^{-10}m^2$ Right: $5.56\times10^{-11}m^2$)

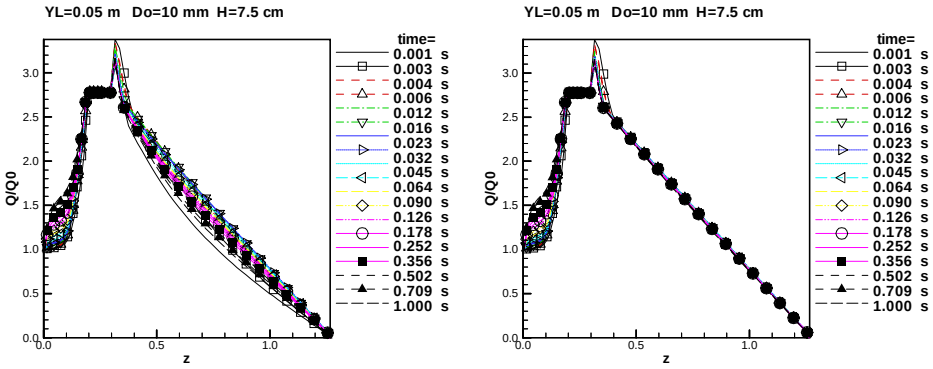

Figure 11 Transient entrainment of gas for different axial inlet velocities (Left: $5.56\times10^{-10}m^2$ Right: $5.56\times10^{-11}m^2$)

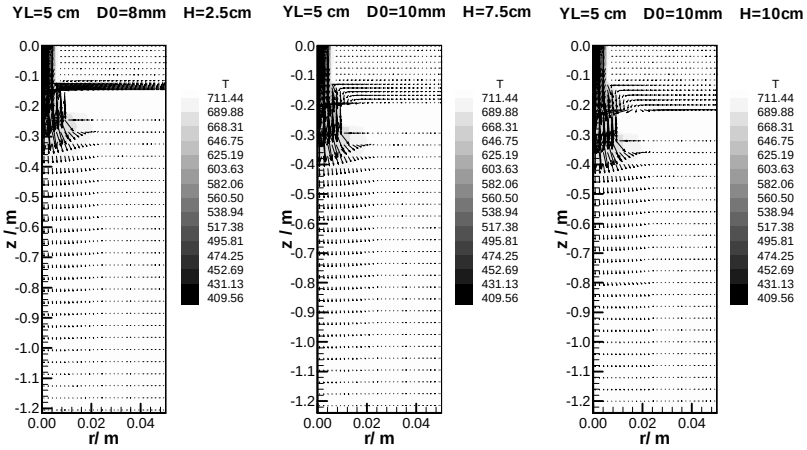

Figure 12 Thermal field for different H